Chem. Chem. Technol., 2020,
Vol. 14, No. 2, pp. 146–153

Chemistry

FERROCENYLMETHYLNUCLEOBASES: SYNTHESIS, DFT CALCULATIONS, ELECTROCHEMICAL AND SPECTROSCOPIC CHARACTERISATION

Elhafnaoui Lanez[1, 2], Lazhar Bechki[2], Touhami Lanez[1, ✉]

https://doi.org/10.23939/chcht14.02.146

Abstract. Three ferrocenylmethylnucleobases (FcMeNb) were synthesized and characterized by cyclic voltammetry, electronic absorption, FT-IR and NMR spectroscopy. The energy of frontier molecular orbitals was determined using DFT/B3LYP method combined with 6-311++G(d,p) basis set in acetonitrile. The lower standard rate constant values of the FcMeNb compounds as compared to ferrocene indicated slower electron transfer kinetics.

Keywords: nucleobases, ferrocene, cyclic voltammetry, Uv-Vis spectroscopy, DFT.

1. Introduction

The discovery of ferrocene and determination of its remarkable stable structure in the 1950's has made a new route for modern organometallic chemistry. In the recent years, ferrocene derivatives chemistry has developed as a rapidly growing and maturing filed which links classical organic chemistry to organometallic chemistry [1, 2]. The stability of the ferrocenyl group of ferrocene derivatives in aqueous solutions, the ease of the synthesis of a large variety of ferrocene derivatives, and its excellent electrochemical properties have made ferrocene derivatives very interesting molecules for biological applications and medicinal chemistry [3, 4]. The chemistry of ferrocenylmethylnucleobases (FcMeNb) [5-9] is still, however, an undeveloped area compared with well-established classical medicinal chemistry of purely organic nucleobase derivatives [10-17]. The first work on the synthesis of FcMeNb was reported by Chen in 1980 [5], who prepared 9N-(ferrocenylmethyl)adenine from the reaction of 6-chloropurine and ferrocenylmethylamine in methoxyethanol. After that many ferrocene-modified nucleosides were described [7, 18]. In addition, the anticancer activity of the FcMeNb was evaluated *in vitro* and *in vivo* using electrochemical and spectroscopic assays [6, 19]. FcMeNb also have been used as a useful set of building blocks for supramolecular chemistry due to their capacity for base-pair hydrogen bonding allied with redox properties [7].

Interest in ferrocenylmethylnucleobases conjugates has increased in the past ten years because of their applications in bioanalytical and medicinal chemistry. For example, all conjugates exhibit *in vivo* antitumor activity [20] but 9N-(ferrocenylmethyl)adenine possesses the highest activity because of its low $E_{HOMO\text{-}LUMO}$ energy gaps, 1-ferrocenylmethylthymine is used as inhibitor of tumor systems [21], and 9N-(ferrocenylmethyl)adenine found its applications as electrochemical sensors [22].

Herein we describe the synthesis, characterisation, DFT calculation, and electrochemical behaviour of three FcMeNb of the type 1-ferrocenylmethylcytosine (FcMeCy), 1-ferrocenylmethylthymine (FcMeTh) and 9N-(ferrocenylmethyl)adenine (FcMeAd). These three compounds were prepared from the reaction of the corresponding nucleobase with (ferrocenylmethyl)trimethylammonium iodide, which can be either obtained commercially or easily prepared according to a known procedure [23].

2. Experimental

2.1. Reagents

Cytosine (99%), thymine (99%), adenine (99%), and tetrabutylammonium tetrafluoroborate (electrochemical grade 99%) were purchased from Sigma-Aldrich, ferrocene (99%) and orthophosphoric acid (85%) were purchased from Alfa Aesar, magnesium sulphate anhydrous (97%) and iodomethane were purchased from Acros Organics, ethanol (95%) and acetic acid (99-100%) were purchased from Biochem Chemopharma Co (Canada). All other reagents used were of analytical grade.

2.2. Procedures

(Ferrocenylmethyl)trimethylammonium iodide was prepared according to the procedure described in [20].

[1] University of El Oued, VTRS Laboratory, B.P.789, 39000, El Oued, Algeria
[2] University of Ouargla, Chemistry Department, PO Box 511, 30000, Ouargla, Algeria
✉ *touhami-lanez@univ-eloued.dz*

General procedure for the synthesis of ferrocenylmethylnucleobases

Nucleobase (2 mmol) was added in small portions to well-stirred solution of trimethylferrocenylmethylammonium iodide (500 mg, 1.3 mmol) in water (70 cm^3). The resulting mixture was then heated at 383–388 K for 6–16 h. Then it was cooled to room temperature. The resulting precipitate was separated by filtration, washed with water to remove any trace of unchanged quaternary ammonium salt and finally chromatographed/ recrystallized to produce the target ferrocenylmethylnucleobase.

1-Ferrocenylmethylcytosine (260 mg, 65 %) was obtained, as described above, from (ferrocenylmethyl)trimethylammonium iodide (500 mg, 1.3 mmol) and cytosine (220 mg, 2 mmol), heating time was 6 h. The product was recrystallized from dimethylformamide to furnish 1-ferrocenylmethylcytosine as yellow leaflets, m.p. 383–385 K. ^{1}H NMR (400 MHz, $CDCl_3$): δ 4.1 (2H, t, β protons of C_5H_4); 4.3 (5H, s, C_5H_5); 4.4 (2H, t, α-protons of C_5H_4); 4.7 (2H, s, CH_2); 5.7 (1H, d, H5); 7.0 (2H, broad s, NH_2) and 7.70 (1H, d, H6). ^{13}C NMR (400 MHz, $CDCl_3$): δ 49.3 (1C, CH_2Fc); 68.5 (2C, -2C, η^5-C_5H_4, β carbons); 69.2 (5C, η^5-C_5H_5); 69.6 (2C, η^5-C_5H_4, α carbons); 85.1 (1C, η^5-C_5H_4); 110.2 (1C, -C=C-); 140.5 (1C, -C-N-); 149.7 (1C, CO); 169.3 (1C, -C=N-).

1-Ferrocenylmethylthymine (105 mg, 25 %) was obtained, as described above, from (ferrocenylmethyl)trimethylammonium iodide (500 mg, 1.3 mmol) and thymine (252 mg, 2 mmol), heating time was 16 h. The product was purified by column chromatography on alumina eluting with a mixture of 9/1 chloroform/ methanol to produce 1-ferrocenylmethylthymine, the product was recrystallized from dimethylformamide as yellow leaflets, m.p. 488 K with decomposition. ^{1}H NMR (400 MHz, $CDCl_3$): δ 3.44 (3H, s, CH_3), 4.23 (2H, t, β protons of C_5H_4), 4.29 (5H, s, C_5H_5), 4.40 (2H, t, α protons of C_5H_4), 4.64 (2H, s, CH_2N), 7.67 (1H, s, H6) and 11.3 (1H, broad s, H3). ^{13}C NMR (400 MHz, $CDCl_3$): δ 12.6 (1C, CH_3); 46.1 (1C, CH_2Fc); 68.2 (2C, η^5-C_5H_4, β carbons); 68.9 (5C, η^5-C_5H_5); 69.1 (2C, η^5-C_5H_4, α carbons); 83.8 (1C, η^5-C_5H_4); 109.4 (1C, -C=C-); 141.3 (1C, -C-N-); 150.7 (1C, -CO); 170.4 (1C, -CO). IR (KBr, ν, cm^{-1}): 3259–2840, 2960, 1750, 1700, 1110, 1010, 950, 880, 825, 480.

9N-(ferrocenylmethyl)adenine (240 mg, 55.5 %) was obtained, as described above, from (ferrocenylmethy) trimethylammonium iodide (500 mg, 1.3 mmol) and adenine (270 mg, 2 mmol), heating time was 6 h. The crude product was chromatographed on neutral alumina using first chloroform and then 1% methanol/chloroform as eluent to yield, 9N-(ferrocenylmethyl)adenine as yellow crystals, m.p. 516 K. ^{1}H NMR (400 MHz, $CDCl_3$): δ 4.1 (2H, t, β protons of C_5H_4), 4.3 (5H, s, C_5H_5), 4.4 (2H, t, α-protons of C_5H_4), 4.7 (2H, s, CH_2), 5.7 (1H, d, H5), 7.0 (2H, broad s, NH_2) and 7.70 (1H, d, H6). ^{13}C NMR (400 MHz, $CDCl_3$): δ 44.8 (1C, CH_2Fc); 68.1 (2C, η^5-C_5H_4, β carbons); 69.8 (5C, η^5-C_5H_5); 69.6 (2C, η^5-C_5H_4, α carbons); 84.7 (1C, η^5-C_5H_4); 110.8 (1C, -C=C-); 142.6 (1C, -C=C-); 151.0 (2C, N-C=N-); 169.8 (1C, -C=N-). IR (KBr, ν, cm^{-1}): 3590–3270, 3130–3090, 1610, 1410, 1110, 1020, 850, 775, 490.

3. Results and Discussion

3.1. Synthesis

Three target FcMeNb were synthesized in two steps from ferrocene. In the first step the well known quarternary salt (ferrocenylmethy)trimethylammonium iodide was prepared *via* the aminomethylation reaction of ferrocene [23], then in the second step the obtained quaternary salt reacted with cytosine, thymine and adenine to produce FcMeCy, FcMeTh and FcMeAd, respectively. Three derivatives were synthesized by the same procedure, which is heating an aqueous mixture of the quarternary salt (ferrocenylmethy)trimethylammonium iodide and the corresponding nucleobase. Cytosine gave a single product which was identified as FcMeCy. In contrast, thymine and adenine produced a mixture of products; the major products were isolated by column chromatography and identified as FcMeTh and FcMeAd, respecttively. The compounds gave analytical data in accordance with reported methods [4, 6], the molecular structures of the obtained compounds are presented in Fig. 1.

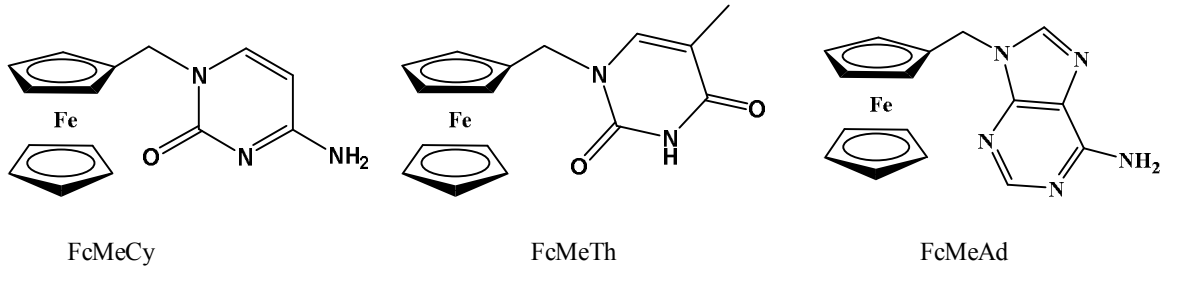

FcMeCy FcMeTh FcMeAd

Fig. 1. Molecular structures of FcMeCy; FcMeTh and FcMeAd

3.2. Cyclic Voltammetry Characterization

Cyclic voltammetry was employed to access electrochemical characteristics of three synthesised FcMeNb. Measurements were performed on a PGZ301 potentiostat/galvanostat (Radiometer Analytical SAS, France) using a three-electrode electrochemical cell of 25 ml containing a glassy carbon (GC) working electrode with a geometric area of 0.013 cm^2, a platinum wire counter electrode of surface area 0.05 cm^2, and an Hg/Hg_2Cl_2 reference electrode (saturated with KCl). The potential was swept starting from -0.2 to +1.2 V with a scanning rate of 100 mV/s. All electrochemical experiments were performed in acetonitrile under nitrogen atmosphere at 298 K. Tetrabutylammonium tetrafluoroborate (Bu_4NBF_4) was used as supporting electrolyte and its concentration was kept 0.1M. The obtained voltammograms are presented in Fig. 2.

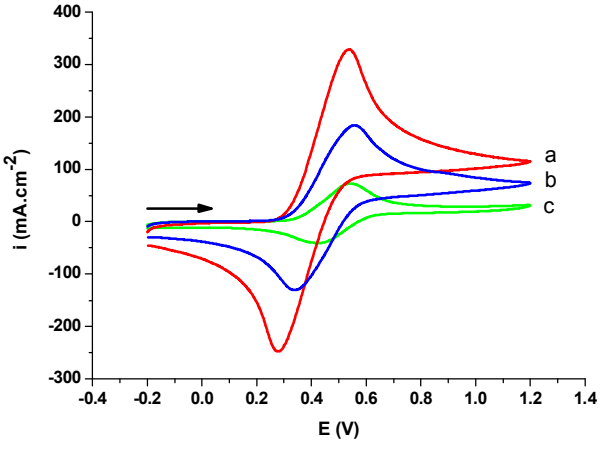

Fig. 2. Cyclic voltammetry of 10 mM FcMeCy (a), FcMeTy (b) and FcMeAd (c) on GC electrode in 0.1M TBATFB/MeCN at scan rate of 0.1 $V{\cdot}s^{-1}$ at 298 K

All voltammograms in Fig. 2 show a couple of well distinct, stable and reversible redox peaks in the studied potential range, the anodic and cathodic peak potentials are summarised in Table 1. The formal potential of FcMeCy, FcMeTh and FcMeAd is greater compared to ferrocene (0.408, 0.447 and 0.482 V *vs.* 0.287 V) under similar conditions. This shift may be explained by the electron withdrawal effect of cytosine, thymine and adenine bases introduced to the cyclopentadienyl ring of ferrocene. The peak to peak separation was, however, considerably higher than the theoretical value of 0.06 V for a totally reversible one-electron processes. This could be due to the uncompensated solution resistance. The anodic and cathodic peak current ratio of approximately 1 is indicative of reversible electrochemical process.

The diffusion coefficient of all FcMeNb in acetonitrile was calculated based on the succession of cyclic voltammograms of Fig. 3 using the following Randles-Sevcik equation (1) [24].

$$ip_a = 2.69 \cdot 10^5 \left(\sqrt{n}\right)^3 SC\sqrt{D}\sqrt{v} \qquad (1)$$

where i is the peak current, A; n is the number of electrons transferred during the oxidation; S is the surface area of the electrode, cm^2; C is the bulk concentration of the electro-active FcMeNb, $mol{\cdot}cm^{-3}$; D is the diffusion coefficient, $cm^2{\cdot}s^{-1}$; and v is the scan rate, $V{\cdot}s^{-1}$.

The plots of the square root of the scan rates versus the anodic peak current density (Fig. 4) suggest that the redox process is diffusion controlled. The values of the diffusion coefficient were deducted from the slope of the linear regression of Eq. (1).

To study the reversible nature of the redox processes and the electron transfer kinetics, the value of standard rate constant of the electron transfer reaction of FcMeNb at the electrode surface were calculated from Nicholson's equation [25]. This equation is derived based on correlation between ΔEp and Ks through a dimensionless parameter ψ:

$$\psi = \frac{Ks}{\sqrt{\pi D \frac{nFv}{RT}}} \qquad (2)$$

where ψ is a dimensionless parameter (depending upon peak separation, ΔEp), it can be obtained from scientific literature [26]; v is the scan rate equal to 100 $V{\cdot}s^{-1}$; D is the diffusion coefficient of the electro-active FcMeNb; F is the Faraday constant equal to 96500 $C{\cdot}mol^{-1}$; n is the number of electrons transferred during the oxidation; R is the gas constant equal to 8.32 $J{\cdot}mol^{-1}K^{-1}$; and T is the absolute temperature of 298 K. The obtained values of Ks are summarized in Table 3.

Table 1

Electrochemical parameters for the oxidation of ferrocene and FcMeNb

Compound	Ep_a, V	Ep_c, V	ip_a, mA	ip_c, mA	ΔEp, mV	E_0, V	ip_a/ip_c
Fc	0.324	0.251	0.259	-0.240	73	0.287	0.85
FcMCy	0.539	0.276	0.326	-0.343	263	0.408	0.95
FcMTy	0.559	0.336	0.183	-0.180	223	0.447	1.02
FcMAd	0.544	0.420	0.072	-0.060	124	0.482	1.2

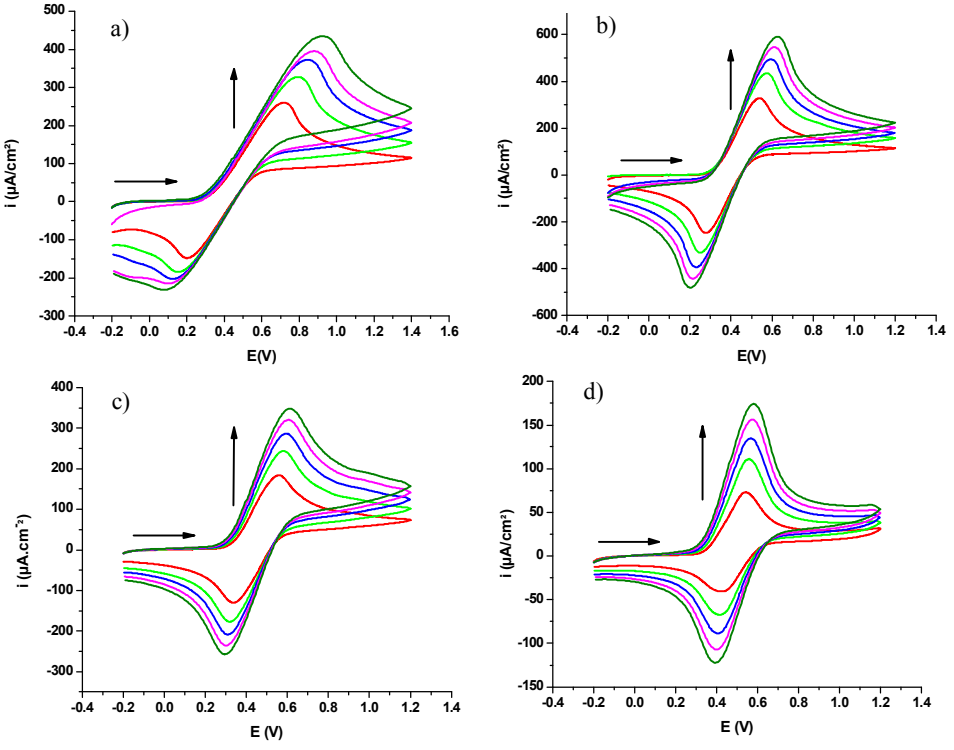

Fig. 3. Cyclic voltammetric behavior of 10 mM Fc (a); FcMeCy (b); FcMeTy (c) and FcMeAd (d) on GC electrode in 0.1M TBATFB/MeCN at scan rates of 0.5, 0.4, 0.3, 0.2, and 0.1 $V \cdot s^{-1}$ at 298 K. The vertical arrowhead indicates increasing scan rate

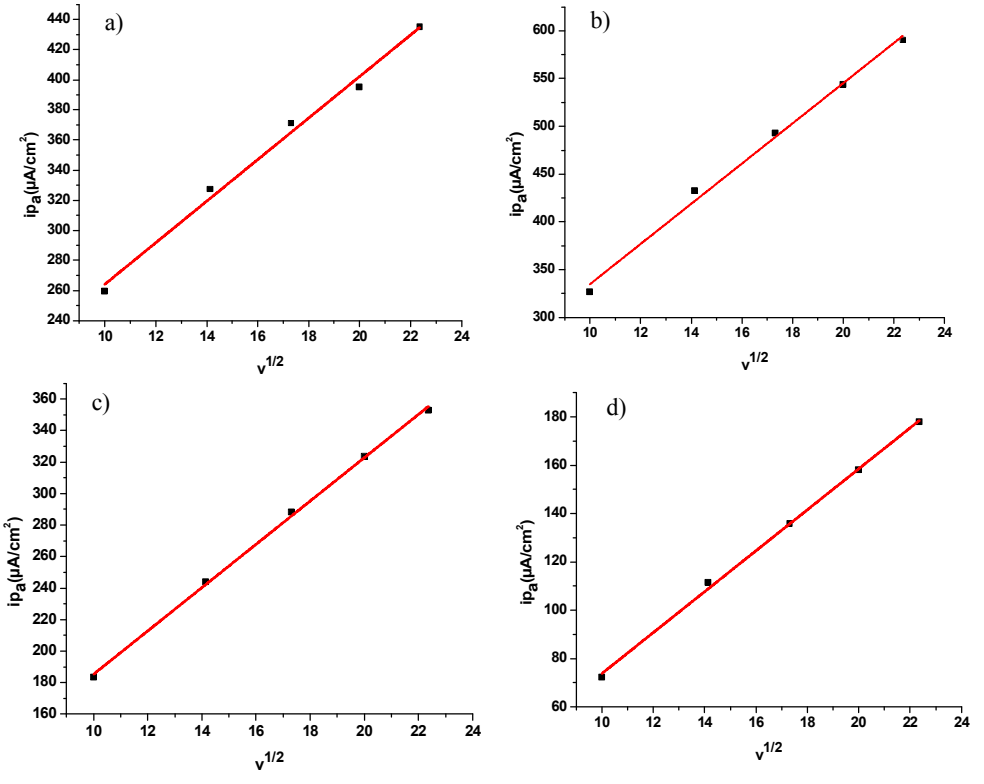

Fig. 4. Plots of $\sqrt{v}$ *versus* ip_a used to calculate the coefficient diffusion

Table 2

Diffusion constants values

Compound	Equation	R^2	$D \cdot 10^{-7}$, cm^2/s
Fc	$y = 13.805x + 126.13$	0.990	1.558
FcMeCy	$y = 21.038x + 124.36$	0.997	3.619
FcMeTy	$y = 13.752x + 147.75$	0.999	3.546
FcMeAd	$y = 11.468x + 10.830$	0.998	2.586

Table 3

Kinetic parameters of Fc and FcMeNb as obtained from electrochemical measurements

Compound	Ψ	ΔEp, mV	$Ks \cdot 10^3$, cm/s
Fc	1.51	73	2.88
FcMCy	0.074	263	0.14
FcMTy	0.100	223	0.19
FcMAd	0.323	124	0.62

The values of *Ks* correspond to the reversible nature of the redox processes with slow electron transfer kinetics. The sequence (Fc > FcMeAd > FcMeTy > FcMeCy**)** of the *Ks* values, indicates that the fast diffusing Fc with no nucleobase is more favorable for electron transfer than compounds FcMeAd, FcMeTy and FcMeCy. The slow electron transfer of FcMeAd, FcMeTy and FcMeCy may be due to the bulky nucleobase attached to the ferrocenyl group.

3.3. Electronic Spectroscopy Characterization

Electronic spectra measurements were conducted on a UV-Vis spectrometer, (Shimadzu 1800, Japan). The spectroscopic response of 10 mM of each FcMeNb in acetonitrile was recorded at 298 K. Typical absorption bands of aromatic ring were observed at 325 and 436 nm for FcMeCy and at 317 and 435 nm for FcMeTy.

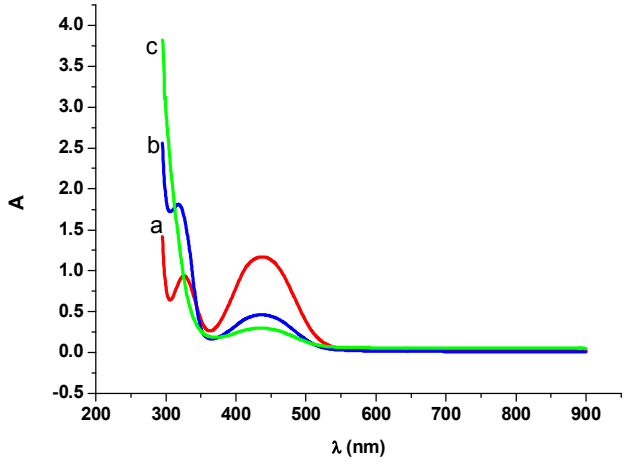

Fig. 5. UV-visible absorption spectra of 10 mM FcMeCy (a), FcMeTy (b) and FcMeAd (c) in acetonitrile at 298 K

Two first bands at 325 and 317 nm correspond to $n \rightarrow \pi^*$ electronic transitions involving the conjugated system (aromatic ring) while the second two bands are attributed to the $\pi \rightarrow \pi^*$ electronic transitions. FcMeAd bears only one typical absorption band at 433 nm which corresponds to $\pi \rightarrow \pi^*$electronic transitions, Fig. 5.

3.4. DFT Calculations

The molecular structure of ferrocene and FcMeNb was optimized at the level of density functional theory (DFT) with DFT/B3LYP method combined with 6-311++G(d,p) basis set in acetonitrile. The molecule was built and optimized using Gaussian 09 program package [27]. The optimised structures of all studied FcMeNb are shown in Fig. 6, and the corresponding calculated bond lengths are tabulated in Table 5.

Fig. 7 shows a schematic representation of the energies of molecular orbitals and contours of lowest unoccupied molecular orbitals (LUMOs) and highest occupied molecular orbital (HOMOs) of the three studied FcMeNb. The HOMO to LUMO energy gap in FcMeCy, FcMeTh and FcMeAd is equal to -4.864, -4.420 and -4.240 eV, respectively. Here it is observed that both the LUMOs and HOMOs are composed of both the ferrocene moiety and the nucleobase orbitals.

Other parameters including separation energies ΔE, absolute hardness η, absolute electronegativities, χ, chemical potentials *Pi*, absolute softness σ, global softness *S*, global electrophilicity Ω, and additional electronic charge ΔN_{max}, have been calculated according to the following equations [28]:

$$\Delta E = E_{LUMO} - E_{HUMO} \quad (3)$$

$$\eta = \frac{\Delta E}{2} \quad (4)$$

$$\chi = \frac{-E_{HUMO} - E_{LUMO}}{2} \quad (5)$$

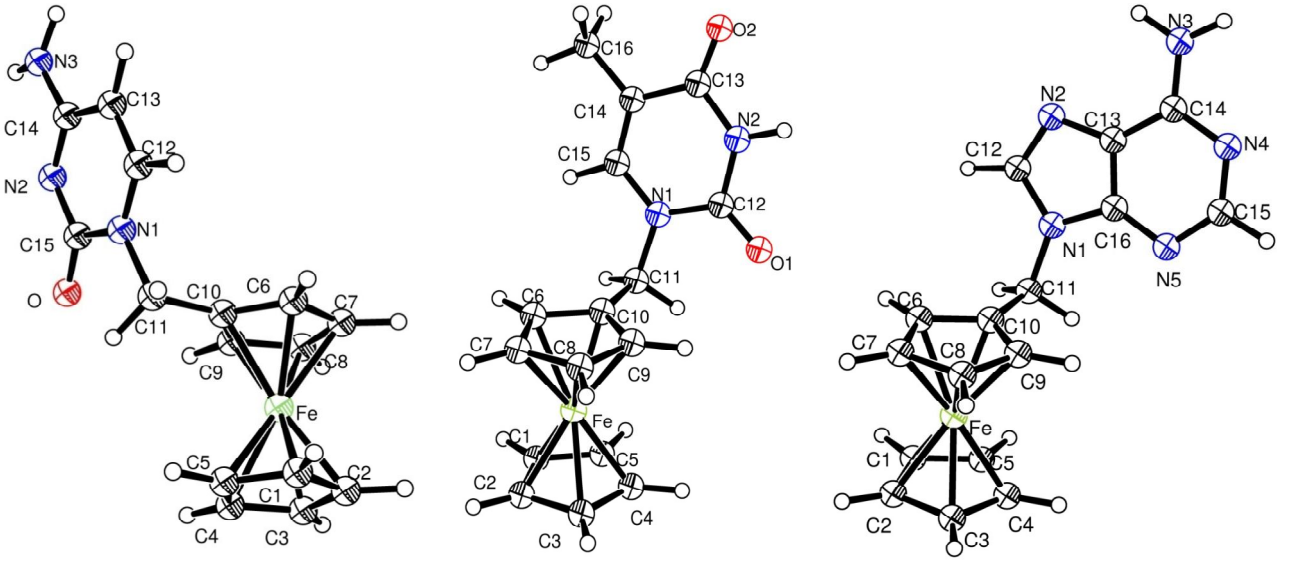

FcMeCy FcMeTy FcMeAd

Fig. 6. ORTEP representation of FcMeCy, FcMeTy and FcMeAd. Displacement ellipsoids are drawn at the 30% probability level and H atoms are shown as small spheres of arbitrary radii

Table 5

List of experimental and calculated bond length values

FcMeCy				FcMeTh				FcMeAd			
FcMeCy				FcMeTh				FcMeAd			
Bond	RX	Cal.	GAP	Bond	RX	Cal.	GAP	Atoms A-B	RX	Cal.	GAP
Fe-C1	2.026	2.079	0.053	Fe-C1	2.036	2.079	0.043	Fe-C1	2.041	2.078	0.037
Fe-C2	2.028	2.078	0.05	Fe-C2	2.036	2.077	0.041	Fe-C2	2.043	2.077	0.034
Fe-C3	2.028	2.076	0.048	Fe-C3	2.045	2.076	0.031	Fe-C3	2.039	2.077	0.038
Fe-C4	2.027	2.077	0.05	Fe-C4	2.047	2.077	0.03	Fe-C4	2.038	2.078	0.04
Fe-C5	2.023	2.078	0.055	Fe-C5	2.035	2.078	0.043	Fe-C5	2.034	2.078	0.044
Fe-C6	2.041	2.071	0.03	Fe-C6	2.031	2.071	0.04	Fe-C6	2.031	2.072	0.041
Fe-C7	2.046	2.075	0.029	Fe-C7	2.045	2.078	0.033	Fe-C7	2.034	2.078	0.044
Fe-C8	2.034	2.079	0.045	Fe-C8	2.047	2.080	0.033	Fe-C8	2.042	2.079	0.037
Fe-C9	2.021	2.075	0.054	Fe-C9	2.038	2.073	0.035	Fe-C9	2.041	2.074	0.033
Fe-C10	2.023	2.070	0.047	Fe-C10	2.026	2.067	0.041	Fe-C10	2.031	2.068	0.037
C1-C2	1.396	1.426	0.03	C1-C2	1.414	1.426	0.012	C1-C2	1.402	1.426	0.024
C1-C5	1.400	1.427	0.027	C1-C5	1.413	1.427	0.014	C1-C5	1.408	1.427	0.019
C2-C3	1.386	1.426	0.04	C2-C3	1.415	1.426	0.011	C2-C3	1.416	1.425	0.009
C3-C4	1.392	1.426	0.034	C3-C4	1.418	1.425	0.007	C3-C4	1.408	1.425	0.017
C4-C5	1.403	1.426	0.023	C4-C5	1.409	1.426	0.017	C4-C5	1.417	1.426	0.009
C6-C7	1.415	1.425	0.01	C6-C7	1.427	1.425	0.002	C6-C7	1.413	1.424	0.011
C6-C10	1.419	1.433	0.014	C6-C10	1.422	1.432	0.01	C6-C10	1.430	1.431	0.001
C7-C8	1.410	1.426	0.016	C7-C8	1.413	1.426	0.013	C7-C8	1.420	1.426	0.006
C8-C9	1.422	1.424	0.002	C8-C9	1.423	1.424	0.001	C8-C9	1.409	1.424	0.015
C9-C10	1.428	1.430	0.002	C9-C10	1.426	1.431	0.005	C9-C10	1.433	1.430	0.003
C10-C11	1.497	1.502	0.005	C10-C11	1.491	1.502	0.011	C10-C11	1.497	1.502	0.005
C11-N1	1.471	1.479	0.008	C11-N1	1.485	1.480	0.005	C11-N1	1.470	1.469	0.001
C12-N1	1.363	1.353	0.01	C12-N1	1.369	1.391	0.022	N1-C12	1.358	1.380	0.022
C12-C13	1.341	1.358	0.017	C12-N2	1.373	1.384	0.011	C12-N2	1.314	1.311	0.003
C13-C14	1.423	1.433	0.01	C12-O1	1.229	1.218	0.011	N2-C13	1.395	1.382	0.013

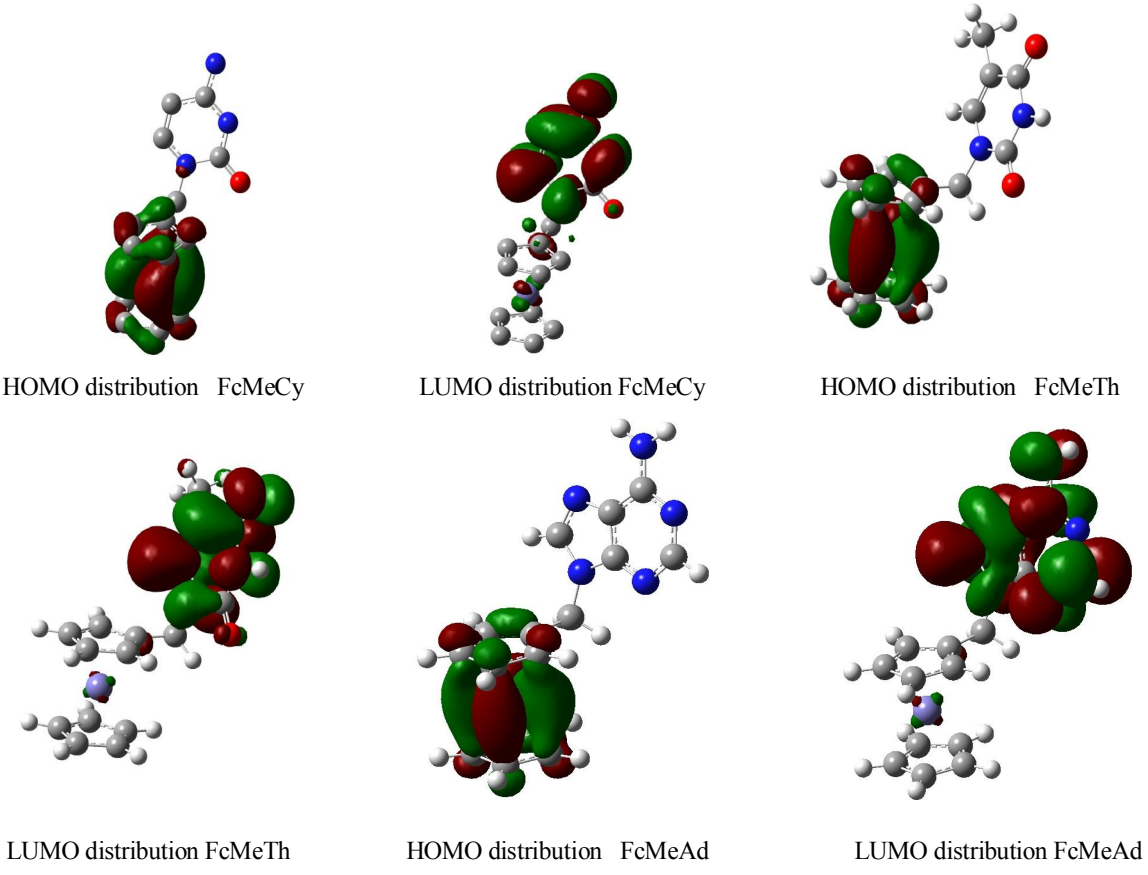

Fig. 7. Representations of HOMO and LUMO for FcMeCy, FcMeTy and FcMeAd determined at B3LYP/6-311++G(d,p) level of theory

Table 4

The calculated quantum chemical parameters for the investigated FcMeNb and ferrocene

Entry	E_{LUMO}	E_{HUMO}	ΔE, eV	η, eV	χ, eV	Pi, eV	σ, eV^{-1}	S, eV^{-1}	Ω eV	ΔN_{max}
Fc	-0.697	-5.632	4.935	2.47	3.1645	-3.16	0.41	0.20	2.03	1.28
FcMCy	-1.305	-5.725	4.864	2.43	3.32	-3.32	0.41	0.21	2.27	1.37
FcMTy	-1.520	-5.760	4.420	2.21	3.51	-3.51	0.45	0.23	2.80	1.59
FcMAd	-1.173	-5.757	4.240	2.12	3.64	-3.64	0.47	0.24	3.12	1.72

$$Pi = -\chi \quad (6)$$

$$\sigma = \frac{1}{\eta} \quad (7)$$

$$S = \frac{1}{2\eta} \quad (8)$$

$$\Omega = \frac{Pi^2}{2\eta} \quad (9)$$

$$\Delta N_{max} = \frac{-Pi}{\eta} \quad (10)$$

The E_{HOMO} values calculated theoretically from DFT were compared with the oxidation peak potentials obtained experimentally from the cyclic voltammetry measurements. The oxidation peak potentials are in the following order: FcMTy > FcMAd > FcMCy, Table 1. This observation was found to be in a good agreement with the electrochemical band gaps supported from the DFT study by comparing the E_{HOMO} values, Table 4. The $E_{HOMO\text{-}LUMO}$ energy gaps were correlated with E_{pa}–E_{pc} potential gap obtained from the difference between the oxidation and reduction peak potential of each compounds (R^2 = 0.574), Fig. 8. The small value of R^2 could be due to the low number of studied samples.

From the DFT calculations it is revealed that FcMeCy, FcMeTh and FcMeAd bond lengths are similar to each other and match well with the experimental values obtained from X-ray crystallographic data [6, 7].

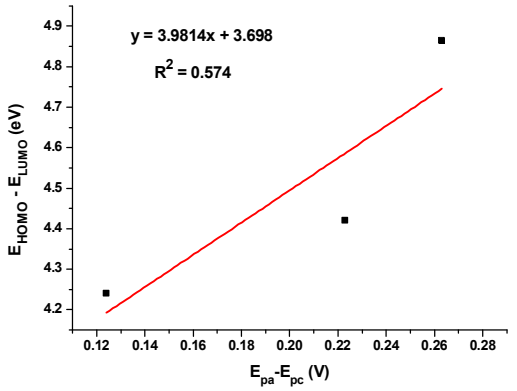

Fig. 8. Linear correlation graph between E_{pa}–E_{pc} potential band gap and E_{HOMO}-E_{LUMO} band gap

4. Conclusions

Three ferrocenylmethylnucleobases were synthesised and structurally characterised by cyclic voltammetry and spectroscopic techniques and have been optimised through DFT calculations in acetonitrile. Redox studies of the compounds in acetonitrile reveal one reversible Fe(II)/Fe(III) oxidative couple. The standard rate constants were determined by the application of Nicholson equation, the lower *Ks* values of the FcMeNb complexes as compared to ferrocene indicated slower electron transfer kinetics. Moreover, the energy of frontier molecular orbitals E_{HOMO} and E_{LUMO} of studied compounds was determined using DFT/B3LYP method combined with 6-311++G(d,p) basis set in acetonitrile. The theoretically calculated E_{HOMO}-E_{LUMO} energies band gap correlates with the potential E_{pa}–E_{pc} band gap determinate from cyclic voltammetry measurements, having a correlation coefficient of 0.574.

Acknowledgements

The authors are grateful to the Algerian Ministry of Higher Education and Research for financial support (project code: B00L01UN390120150001). We would also like to thank Mr Ali Tliba (VTRS staff) for his help.

References

[1] Khand U., Lanez T., Pauson P.: J. Chem. Soc., Perkin Trans., 1989, **1**, 2075. https://doi.org/10.1039/P19890002075
[2] Lanez T., Pauson P.: J. Chem. Soc., Perkin Trans., 1990, **1**, 2437. https://doi.org/10.1039/P19900002437
[3] Larik A., Saeed A., Fattah T. *et al.*: Appl. Organomet. Chem., 2017, **31**, 1. https://doi.org/10.1002/aoc.3664
[4] Santos M., Bastos P., Catela I. *et al.:* Mini-Rev. Med. Chem., 2017, **17**, 771. https://doi.org/10.2174/1389557516666161031141620
[5] Chen S.: J. Organomet. Chem., 1980, **202**, 183. https://doi.org/10.1016/S0022-328X(00)90515-1
[6] Price C., Aslanoglu M., Isaac J. *et al.*: J. Chem. Soc., Dalton Trans., 1996, **21**, 4115. https://doi.org/10.1039/DT9960004115
[7] Houlton A.; Isaac C.; Gibson A. *et al.*: J. Chem. Soc., Dalton Trans., 1999, **18**, 3229. https://doi.org/10.1039/A905168F
[8] Kowalski K., Szczupak Ł., Saloman S. *et al.*: ChemPlusChem., 2016, **82**, 303. https://doi.org/10.1002/cplu.201600462
[9] Kowalski K.: Coordin. Chem. Rev., 2016, **317**, 132. https://doi.org/10.1016/j.ccr.2016.02.008
[10] Hocek M.: Eur. J. Org. Chem., 2003, **2**, 245. https://doi.org/10.1002/ejoc.200390025
[11] Gundersen L., Nissen-Meyer J., Spilsberg D.: J. Med. Chem., 2002, **45**, 1383. https://doi.org/10.1021/jm0110284
[12] Cocuzza A., Chidester D., Culp S. *et al.*: Bioorg. Med. Chem. Lett., 1999, **9**, 1063. https://doi.org/10.1016/S0960-894X(99)00133-X
[13] Chiosis G., Lucas B., Shtil A. *et al.*: Bioorg. Med. Chem., 2002, **10**, 3555. https://doi.org/10.1016/S0968-0896(02)00253-5
[14] De Clercq E., Holy A., Rosenberg I. *et al.*: Nature, 1986, **323**, 464. https://doi.org/10.1038/323464a0
[15] Wagstaff A., Faulds D., Goa K.: Drugs, 1994, **47**, 153. https://doi.org/10.2165/00003495-199447010-00009
[16] Zhao L., Zhang L., Liu J. *et al.*: Eur. J. Med. Chem., 2012, **47**, 255. https://doi.org/10.1016/j.ejmech.2011.10.050
[17] Cho Y., Lee J., Song S.: Bioconjug. Chem., 2005, **16**, 1529. https://doi.org/10.1021/bc049697u
[18] Meunier P., Quattara B., Gautheron J. *et al.*: Eur. J. Med. Chem., 1991, **26**, 351. https://doi.org/10.1016/0223-5234(91)90070-4
[19] Lanez E., Bechki L., Lanez T.: Chem. Chem. Technol., 2019, **13**, 11. https://doi.org/10.23939/chcht13.01.011
[20] Neuse E.: J. Inorg. Organomet. Polym. Mater., 2005, **15**, 3. https://doi.org/ 10.1007/s10904-004-2371-9
[21] Simenela A., Morozova E., Snegura L. *et al.*: Appl. Organomet. Chem., 2008, **23**, 219. https://doi.org/10.1002/aoc.1500
[22] Sun R., Wang L., Yu H. *et al.*: Organometallics, 2014, **33**, 4560. https://doi.org/10.1021/om5000453
[23] Osgerby J., Pauson P.: J. Chem. Soc., 1958, **642**, 656. https://doi.org/10.1039/JR9580000656
[24] Brett C., Brett A.: Electrochemistry: Principles, Methods and Applications. Oxford Science University Publ., Oxford 1993.
[25] Nicholson R., Shain I.: Anal. Chem., 1964, **36**, 706. https://doi.org/10.1021/ac60210a007
[26] Nicholson R., Shain I.: Anal. Chem., 1965, **37**, 1351. https://doi.org/10.1021/ac60230a016
[27] Frisch M., Trucks G., Schlegel H. *et al.*: Gaussian 09. Gaussian Inc., Wallingford CT, 2009.
[28] Pearson R.: J. Am. Chem. Soc., 1963, **85**, 3533. https://doi.org/10.1021/ja00905a001

Received: August 16, 2018 / Revised: October 17, 2018 / Accepted: January 12, 2019

ФЕРРОЦЕНІЛМЕТИЛНУКЛЕЇНОВІ ОСНОВИ: СИНТЕЗ, РОЗРАХУНОК ДПФ, ЕЛЕКТРОХІМІЧНА ТА СПЕКТРОСКОПІЧНА ХАРАКТЕРИСТИКА

Анотація. *Синтезовані три ферроценілметилнуклеїнові основи (FcMeNb). За допомогою методів циклічної вольтамперометрії, абсорбційної електронної спектроскопії, Фур'є-спектроскопії та ЯМР-спектроскопії охарактеризовано синтезовані сполуки. Енергію прикордонних молекулярних орбіталей визначено за методом DFT/B3LYP у поєднанні з базовим набором 6-311++G(d, p) в ацетонітрилі. Встановлено, що нижчі стандартні константи швидкостей сполук FcMeNb порівняно з ферроценом вказують на більш повільну кінетику переносу електронів.*

Ключові слова: *нуклеїнові основи, ферроцен, циклічна вольтамперометрія, УФ-спектроскопія, ДПФ.*